The isotopic signatures of CO

in

biomass burning emission

MSc thesis

Author:

Chenxi Qiu

Supervisor:

Dr. M. E. Popa

2nd Examiner:

Prof. dr. T. Röckmann

Institute of Marine and Atmospheric research Utrecht

Utrecht University

2 August 2019

Acknowledgement

This work would not have been possible without the wholehearted support from my supervisor, Elena Popa. I am grateful to all of those with whom I have had the pleasure to work and from whom I received great help and advice. The people to whom I would like to pay my special tributes include but are not limited to Carina van der Veen, Dusan Materic, Henk Snellen, Rupert Holzinger, Sophie Hietbrink, Thomas Röckmann from IMAU, Utrecht University; Anupam Shaikat, Henk Jansen, Peng Yao, Marcel de Vries, Ulrike Dusek from Centre for Isotope Research, University of Groningen; Guido van der Werf , Hans Cornelissen , Patrik Winiger, Roland Vernooij from VU Amsterdam.

Abstract

This study aims to better characterize fire emissions by examining biomass burning emissions of carbon monoxide, carbon dioxide, organic carbonaceous aerosols and their isotopic compositions, as well as of volatile organic compounds (VOCs). What has been poorly known and what this study focuses on is how combustion efficiency and fuel moisture affect emissions and the link between organic carbonaceous aerosol and gaseous emissions. The results show significant isotopic fractionation in the production of both CO and CO2. Isotopes in CO and CO_2 are strongly associated with combustion efficiency and with burning phases. A clear pattern is found between CO isotopic ratios and modified combustion efficiency (MCE). Both $\delta^{13}C$ and $\delta^{18}O$ increase with increasing MCE until both isotopic ratios reach maximum when the combustion is close to complete. Results confirmed the decreasing trend of $\delta^{13}C$ and $\delta^{18}O$ in CO over time from ignition during a whole combustion process, along with decreasing MCE. Similar depletion trend was also found in CO_2. $\delta^{13}C$ in organic carbonaceous aerosol is largely correlated with $\delta^{13}C$ in CO, but such correlation is completely absent in the flaming phase of fire. Fuel moisture may affect burning emission, but the results suggest the effect may be small. VOC emissions remain uncertain concerning the quantities emitted and the timings of emissions. The preliminary results in this study can potentially lead to better characterization for the isotopic compositions of CO emission according to combustion efficiency.

Contents

1 Introduction

1.1 Open Biomass burning

Open biomass burning is an important source of atmospheric trace gases and aerosols influencing the atmospheric composition (Andreae, 2019). Although subject to seasonality and year-to-year variability, open biomass burning has impacts on local, regional and global air quality as well as on global radiation budget (Wiedinmyer et al., 2011). Direct radiative forcing of climate from the contribution of biomass burning, despite its significance, is poorly quantified (Ramaswamy et al., 2001). As part of the global carbon cycle, open biomass burning plays an important role in mobilizing carbon from the biosphere to the atmosphere. According to the estimate of van der Werf et al. (2010) by adopting biogeochemical model and satellite observations for year 1997 to year 2009, the annual global fire carbon emissions vary from 1.5 to 2.8 Pg C $year^{-1}$. Most of this carbon exchange is in the form of CO_2. As for CO emission, open biomass burning emission alone makes up of about one-third to one-half of the total surface source for CO (Andreae, 2019). In the tropics, biomass burning is the most important source of CO (Crutzen and Carmichael,1993). Emissions of carbon-containing volatile organic compounds (VOCs) and carbonaceous aerosols from biomass burning have impacts on atmospheric chemistry environment and aerosol optical depth (Gaeggeler et al., 2008). The source strengths of VOCs and carbonaceous aerosols from biomass burning, however, are largely unclear. Wildfires, as an important part of open biomass burning have strong geographical and seasonal distributions.

Amazonia, as one of the most important geographical areas where seasonal wildfires take place, potentially exerts influence on the global scale (Levine, 1996). Amazonian wildfire events on average peak between July and November. Previous studies have shown such wildfire events and their emissions over the Amazonia. However, emissions vary greatly owing to climate variability, particularly ENSO-related drought events (e.g. van der Werf et al., 2008; van der Laan-Luijkx et al., 2010; Alencar et al., 2011).

1.2 Carbon monoxide

Carbon monoxide (CO) plays an important role in tropospheric chemistry. The background volume mixing ratio of CO in troposphere observed can be as low as 35 part per billion

(ppb) over summer Antarctica to as high as 200 ppb in winter northern hemisphere (Röckmann et al., 2002). Nearly all atmospheric CO molecules are eventually removed through oxidation by hydroxyl radical (OH) in reaction $CO+OH=CO_2 + H$. Such oxidation process consumes 60% of the total turnover of OH (Crutzen and Zimmermann, 1991) and therefore CO serves as the major sink for OH. The highly reactive OH is responsible for oxidation of the vast majority of reduced and partly oxidized atmospheric species. Therefore, CO indirectly influences the overall atmospheric oxidation efficiency. CO is also considered an indirect greenhouse gas since CO competes with methane (CH_4), a major greenhouse gas for OH in the oxidation process while such oxidation with OH acts as the main sink for CH_4. In general, more CO leads to higher CH_4 mixing ratio, resulting in higher positive radiative forcing. Additionally, the reaction of CO with OH under high NOx condition can also lead to ground-level ozone pollution in urban areas (Westberg et al., 1971), triggering a variety of health problems for humans.

Despite its significance, the budget of CO is still poorly characterized with error bar for total source strength larger than 100% of the average value. A large part of the uncertainty comes from biomass burning, which this study is aimed to contribute to improve.

Table 1:

The global tropospheric budget of CO (Brenninkmeijer et al., 1999).

Sources	Strength (Tg/yr)
Fossil fuel combustion	300-550
Biomass burning	300-700
Methane oxidation	400-1000
NMHC oxidation	200-600
Ozonolysis	80-100
Biogenic	60-160
Oceans	20-200
Total sources	**1800±2700**
Sinks	Strength (Tg/yr)
Oxidation by OH	1400-2600
Soil uptake	250-640

Transport to stratosphere	200-600
Total sinks	**2100±3000**

1.3 Stable Isotope analysis

1.3.1 Background

Stable isotope analysis will be applied to study the CO and CO_2 emission. Isotopes are atoms which have the same number of protons, i.e. atomic number, but differ in the number of neutrons and thus in mass number. The Isotopologues are molecules that only differ in their isotopic composition. For carbon element, the stable isotopes found in nature are carbon-12 (^{12}C) and carbon-13 (^{13}C) with natural abundance of 98.9% and 1.1% respectively. For oxygen element, the stable isotopes are oxygen-16 (^{16}O), oxygen-17 (^{17}O) and oxygen-18 (^{18}O) with natural abundance of 99.76%, 0.04% and 0.20% respectively. Due to the low abundance and small variation in secondary isotopes, the isotopic ratio is commonly expressed in terms of parts per thousand difference from a standard. This is known as the delta value (δ) in per mill (‰). The value can be measured by mass spectrometry and then compared to the international standards. δ value quantifies the extent to which a sample is enriched or depleted in a certain secondary isotope relative to a reference. Mathematically, it is expressed as

$$\delta = \left(\frac{R_{sample}}{R_{standard}} - 1\right) \cdot 1000‰ \quad (1)$$

In which R is the abundance ratio between the secondary isotope of interest and the most abundant isotope in the sample or by the international standard. What is relevant in this study are the ratio between ^{13}C and ^{12}C and the ratio between ^{18}O and ^{16}O. For ^{13}C, the international standard is Vienna Pee Dee Belemnite (VPDB) and for ^{18}O Vienna Standard Mean Ocean Water (VSMOW).

1.3.2 Stable isotopic analysis for CO

Stable isotope measurement serves as a good supplement for concentration measurement in constraining the budgets of atmospheric trace gases. CO in a given air sample can ideally be apportioned to its sources, given that different sources have distinctive isotopic signatures and the number of sources is not larger than the number of independent variables

(Brenninkmeijer et al., 1999). The isotopic signatures of different CO sources are shown in Table 2. CO has four sources, in which some sources have similar isotopic ratios.

Table 2

The isotopic signatures of various sources of CO (Röckmann et al., 2002)

Sources	$\delta^{13}C$ (‰, VPDB)	$\delta^{18}O$ (‰, VSMOW)
Fossil fuel combustion	-27.5	23.5
Biomass burning	-22.9	17.2
Methane oxidation	-51.1	0
Nonmethane hydrocarbon	-32.2	0
Atmospheric composition	-28 to -23	0 to 10

For atmospheric CO, the oxidation process of CO by OH radicals leads to isotope fractionation, i.e. different reaction rates for different isotopomers. The fractionation factor depends on pressure and can become negative (Röckmann et al., 1998). Isotope ratios in CO also give information about sink processes that influence the distribution of CO through kinetic isotope effect in the atmosphere.

Isotope analysis can also reveal isotopic signature source from which emission has been mixed with background air by using the Keeling plot (Keeling et al., 1989). Source signatures can be implemented into models helping us learn more about the CO budget. Better-defined source isotopic signatures of CO are therefore urgently needed.

1.3.3 Isotopes in CO and CO_2 from biomass burning

Although $\delta^{13}C$ in atmospheric CO_2 is about -8‰ in absence of any industrial activities, biomass is depleted in $\delta^{13}C$, ranging from -27‰ to -13‰, due to the isotopic fractionation towards lighter ^{12}C in CO_2 uptake. Two main types of photosynthesis lead to two groups of plants of distinct carbon isotopic compositions, i.e. C3 and C4 plants. The majority, about 95% of plants on earth are C3 while around 5% of the plants are C4. $\delta^{13}C$ is on average -27‰ for C3 plants and -13‰ for C4 plants (O'Leary, 1981; Farquhar et al., 1989).

Isotopes in CO and CO_2 emissions from biomass burning also reflect the difference between these two groups. CO_2 as the main carbon emission species, largely represents the isotopic ratios of the biomass and therefore the difference is similar to the difference in

biomass. CO, however, has much higher variation. One laboratory study conducted by Kato et al. (1999b) has shown that $\delta^{13}C$ and $\delta^{18}O$ in CO emission could vary by up to around 8‰ and 12‰ respectively throughout one single fire, with heavier CO in the flaming phase and lighter CO in the smoldering phase for both carbon and oxygen. The main limitation of Kato's study is that only isotopes in CO are revealed, but how isotopes in CO_2 changes throughout the fire has not been studied.

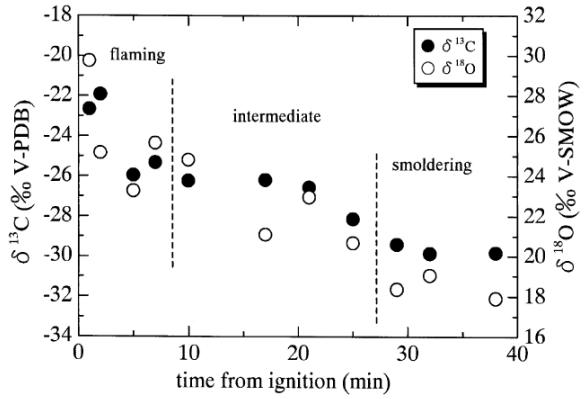

Fig.1. CO isotopic compositions from eucalyptus branches burning emission as a function of time from ignition. (figure from Kato et al., 1999b)

1.4 Carbonaceous aerosols and biomass burning

Biomass burning is a major source of carbonaceous aerosols in the atmosphere (van der Werf et al., 2010), which affect both climate and air quality due to their size, optical and chemical properties (e.g. Lelieveld et al., 2015). Organic carbon (OC) fraction and black or elemental carbon (BC or EC) fraction are the two components into which carbonaceous aerosol is commonly divided. Previous studies have shown difficulties in quantifying OC (Fuzzi, 2006), of both primary and secondary source (i.e. formed through gas-to-particle conversion in the atmosphere). Reasons for the poor quantification of primary OC is the lack of knowledge in the chemical compositions of OC and its characteristic emission profiles (Pio et al., 2011). Such uncertainties in primary source of OC makes it even more difficult to quantify OC of secondary source. In particular, the relationships between primary OC and gaseous species from biomass burning are largely unknown. $PM_{2.5}$ is defined as particles with aerodynamic diameter smaller than 2.5 μm. Numerous evidences have indicated the adverse effects of $PM_{2.5}$ on human health (e.g. Dominici et al., 2006). Several studies have shown that carbonaceous content represents an important part of $PM_{2.5}$

particles, constituting 21-78% of the mass fraction (Pio et al., 2011) and biomass burning emission is the largest source of primary (i.e. emitted in particulate form) carbonaceous aerosols (Andreae and Rosenfeld, 2008). Few studies were done in $PM_{2.5}$ from biomass burning and its potential implications.

1.5 Fuel moisture content on emissions

One preliminary laboratory fire study by Chen et al. (2010) has shown that fuel moisture content may play an important role in carbon partitioning in biomass burning emissions. According to this study, emission factors of $PM_{2.5}$ and OC increase with increasing fuel moisture content. OC emission, in some cases, can increase up to 4 times the amount of CO in terms of carbon, indicating fuel moisture may intensify primary production of OC from plant material. How fuel moisture content affects emission is, however, still largely unknown. More studies need to be done, especially in studying the isotopic compositions of OC and main biomass burning emission species CO and CO_2 with varying fuel moisture.

1.6 Controlled fire experiments

In this study, controlled fire experiments will be adopted to study fire emissions. Despite some disadvantages compared to field campaigns (Andreae, 2019), laboratory studies still provide some unique information about biomass burning emission that otherwise cannot be obtained for several reasons.

-First, in the laboratory experiments, we can quantify and vary individual variables of interest one at a time, e.g. moisture contents of the fuel, while controlling other variables.

-Secondly, the success of field campaigns is highly subject to uncertainties in the unconstrained natural conditions, while laboratory emulation is not.

-Thirdly, sampling of some emission species is intrinsically challenging in real field campaigns. This is especially the case for aerosol sampling, which involves pumping air at a specific flow rate through the pre-treated filter and temperature-specific storage of filters.

- Lastly, some biomass burning species like CO_2 have enormous surface sources and sinks, which makes it a challenge to have accurate estimates from the burning in the field.

2 Project outline

The focus of this study is to characterize CO isotopic composition in biomass burning emission. The project was mainly conducted under the laboratory setting in controlled fire facility. Along with CO, emissions of CO_2, carbonaceous aerosol and VOCs from fire were also studied, with special emphasis on the relationships of isotopic compositions of CO, CO_2 and the organic fraction (OC) of carbonaceous aerosols. Moreover, the influence of burning condition, fuel moisture content on emissions were also studied. Three main sets of laboratory experiments were organized. Samples from Amazon flight campaign were studied for CO isotopes. Fuel used in this study included fine fuels of willow wood chips (C3), corn silk (C4) and the 1:1 mixture of the two above, prunus avium wood chunks (C3). Fuel moisture of the fuel ranged from nearly negligible to 24%. Separate studies on the emissions of flaming and smoldering were conducted.

3 Method

3.1 sampling

3.1.1 Air Sampling

Instead of the in-situ method to analyze air samples, we chose to sample the air of interest first in the air containers, inside which air is proven to be chemically stable for the species of interest. We then measured the samples in the laboratory. CO isotopes still fail to achieve such resolution that the intricate differences in isotope ratio can be revealed. Besides limitations in resolution, measurement of isotopic composition is usually done with extremely delicate analytical instruments of considerable size and weight, that are hardly movable.

The air containers used for this study were pressure resistant 1 L glass flasks (provided by Normag® in Germany, Fig. 2). They were covered with opaque rubber to block light. The PCTFE seals of the flask around the two openings were used. Prior to use, the flasks went through ultra-cleaning procedure to ensure no contaminations from previous samples. Such procedure consisted of evacuation, continuous nitrogen flush and final evacuation under 50 °C in the oven for a total of five hours. The final vacuum pressure in the flask was on the scale of 10^{-5} mbar with high vacuum pump (provided by Pfeiffer Vacuum® in Germany).

Before sample air entered the flask, the air must go through a dryer and a particulate filter (Fig. 2). The dryer was a plastic tubing filled with magnesium perchlorate ($Mg(ClO_4)_2$), a drying agent that quantitatively retains water from the air flow in the tube. The drying agent was held in place by glass wool on both ends. After the air was dried, it went through a 7-micron stainless steel particulate filter (provided by Swagelok® in USA). The dry, large particulate-free sample was then collected in the flask.

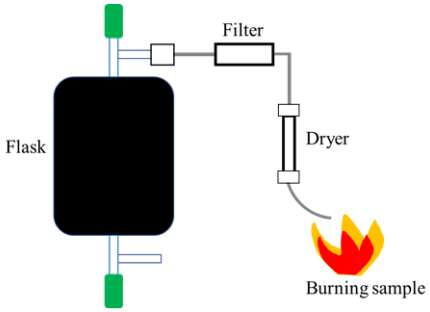

Fig. 2. The set-up for sampling with flask: 1) the pre-vacuumed glass flask as the container for the air sample, 2) 7-micron stainless steel particulate filter to filter out large particles, 3) dryer filled with $Mg(ClO_4)_2$ to remove water vapor.

3.1.2 Aerosol sampling

The filters used in this study were quartz-fiber filters, with the advantage of high heat (well above 800 °C) resistance. The particle size collected was $PM_{2.5}$. The flow rate of the air passing through the filter was 3.5L/min. To avoid evaporation and chemical reactions of OC, the filters were stored at temperature of -30 to -20 °C between sampling and measurement.

3.2 Controlled fire experiments

The controlled fire experiments were conducted in FLARE fire lab at Vrije Universiteit Amsterdam, the Netherlands. The simple set-up consists of a chamber with an exhaust hood on top(Fig. 3c ③), a metal plate to hold the fuel(Fig. 3c ①), a filter to collect aerosol samples(Fig. 3c ②), a pump with one inlet and one outlet (Fig. 3c ⑤), a mass flow controller (MFC) to control the flow rate at which the air entered the filter(Fig. 3c ④), and a Tedlar® sample bag (provided by SKC in Pennsylvania, USA) in the outlet of the pump for air samples(Fig. 3c ⑥). To start sampling, a new filter was first put in place. After setting the flow rate 3.5L/min for MFC, we turned on the pump, so that the air was sucked through the filter to the sample bag. With this novel method, we could sample aerosol and

air samples simultaneously. After finishing each sampling, we took the filter out and relocated the air sample in the sample bag to the glass flask for longer storage. Blanks were taken in the same way, but in absence of burnings.

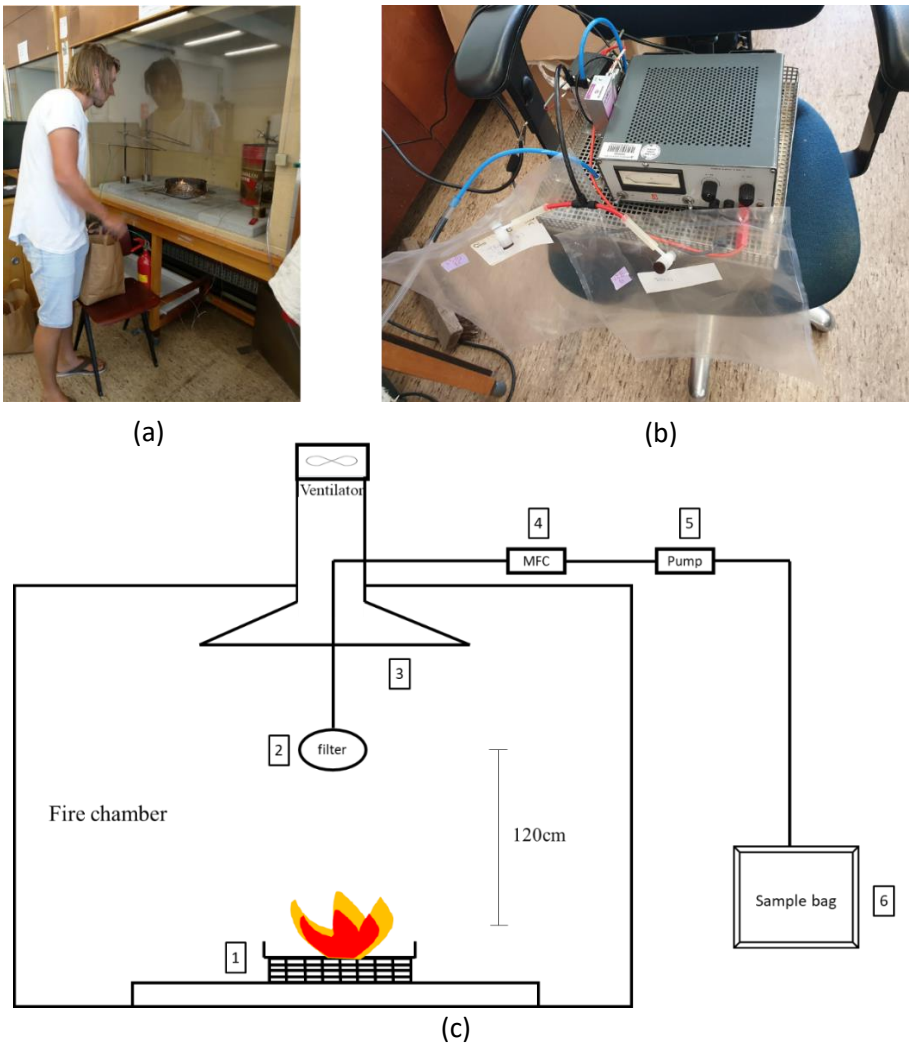

Fig. 3. a) Photo of the fire chamber. b) Photo of the MCF, pump and sample bags. c) The fire chamber set-up consists of 1) metal plate with holes to place the fuel on, 2) quartz fiber filter with pore size for $PM_{2.5}$, on which aerosols stay whereas through which the gas passes 3)exhaust hood, 4) mass flow controller whose flow is set to 3.5L/min to facilitate $PM_{2.5}$ sampling, 5) pump sucking the air to maintain the flow, and whose outlet is connected to the sample bag, 6) Tedlar® sample bag collects the air from the outlet of the pump before the air is relocated to the glass flask.

3.3 Treatment of fuel

To have wood fuel of the same source but different moisture contents, wood needs some special treatment to gain or lose moisture. First, we needed to know the water contents of the untreated original wood. The method was to bake the fuel in oven under 90 °C for days

until the weight was not changing anymore. The water contents were then derived from the weight changes. The treatment to vary moisture contents of the original fuel in this study was to soak the untreated wood until it gained considerable weight, and then to bake the wet wood in oven under 90 °C. Different baking time resulted in different moisture contents of the wood. The weight gain before and after the procedure, combined with the information about the moisture contents of the original fuel were enough to calculate the new moisture contents.

3.4 Measurement systems

3.4.1 continuous-flow isotope-ratio mass spectrometry

The continuous-flow isotope-ratio mass spectrometry system is the gas chromatography/ isotope- ratio mass spectrometry (GC/IRMS) system specially designed for measuring the isotopic compositions in both CO and CO_2 from atmospheric samples of wide range of concentration. The $\delta^{13}C$ and $\delta^{13}C$ and the mixing ratios of CO and CO_2 can be retrieved from the output of the system. An earlier version of the instrument is discussed in detail in Pathirana et al. (2015). Sample loops were added enabling the instrument to measure samples of high concentration, typical for burning samples in this study. The range of concentrations of CO and CO_2 the instrument can measure are up to approx. 1% and 16% respectively. Details about sample loops and selectors are discussed in Appendix A.

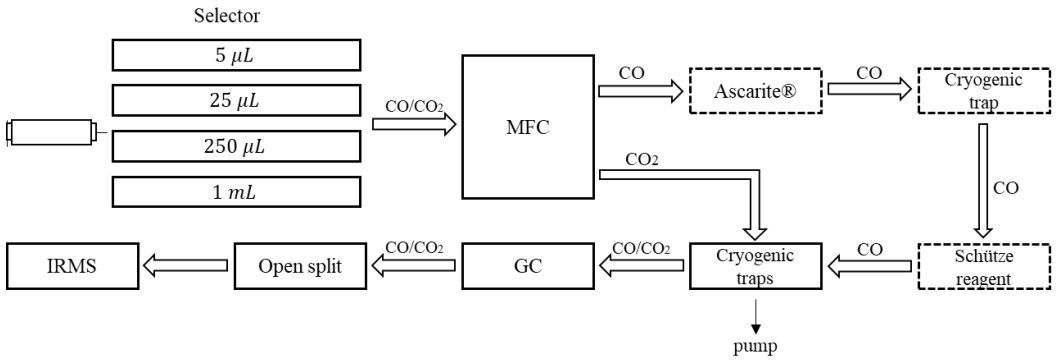

Fig.4. Schematic graph of the continuous-flow isotope-ratio mass spectrometry system: Solid components represent the parts only used for CO measurement. Solid components represent the parts shared by both CO and CO_2 measurement

The system's two measurement modes: CO measurement and CO_2 measurement follow slightly different procedures (Fig. 4). The IRMS is set to measure isotopic compositions in CO_2, which is the common choice for working gas to maintain high precision. While CO_2 can be measured directly by IRMS, CO must be converted to CO_2 first.

For CO measurement, I followed the steps below:

S1: Use syringe to take sample from the flask and then inject the sample into the selector when the right sample loop size is chosen. Only this step is done manually.

S2: Sample is injected into the system with zero air (synthetic air composed of nitrogen and oxygen) while the flow rate and injection time are controlled by MFC.

S3: The sample goes through Ascarite® where CO_2 present in the sample is removed to prevent CO_2 in the sample from being added on the signal of CO-converted CO_2 and influencing the results.

S4: The sample goes through a cryogenic trap in liquid nitrogen temperature (-196 °C) to further condense and remove CO_2, N_2O, water vapor among many other compounds.

S5: The sample goes through Schütze reagent where CO present in the sample is quantitatively converted to CO_2.

S6: CO_2 in the sample is condensed and collected in a steel cryogenic trap in liquid nitrogen while other atmospheric compounds are evacuated by the pump. Then the CO_2 in the trap is transferred to another cryogenic trap made of capillary line to decrease the volume before it enters the GC/IRMS system.

Every time before sample reaches IRMS, CO_2 working gas from the cylinder of known isotopic composition was used as internal reference. In addition, measurements of blank and reference gas of known isotopic composition were measured frequently during sample measurements to ensure maximum accuracy.

3.4.2 Carbonaceous aerosol ^{13}C IRMS measurement

The Carbonaceous aerosol ^{13}C IRMS measurement was conducted at Centre for Isotope Research, University of Groningen, the Netherlands. For each sample measurement, the filters were first cut into 1.5 cm^2 or 1 cm^2 piece(s), depending on its total carbon mass

concentration (that of EC and OC, in μg C/cm^2) on the filter. For optimal performance of the instrument, TC content (in μg C) of the sample put in the oven each time should be in the range of approx. 5 to 20μg.

OC and EC fractions were thermally derived in Sunset® oven (provided by Sunset Laboratory Inc. in USA) in oxygen mode and $\delta^{13}C$ in OC was measured in the form of CO_2. After each sample was pushed in, it first underwent 330 °C to fully mobilize carbon in OC fraction in the form of CO_2, whose amount was monitored by the Sunset® oven. CO_2 emitted here then entered GC/IRMS for $\delta^{13}C$ measurement. The rest of carbonaceous aerosol, EC was released afterwards at 850 °C in the oven and its amount was also monitored by the oven. The whole burning process lasted approximately 13min.

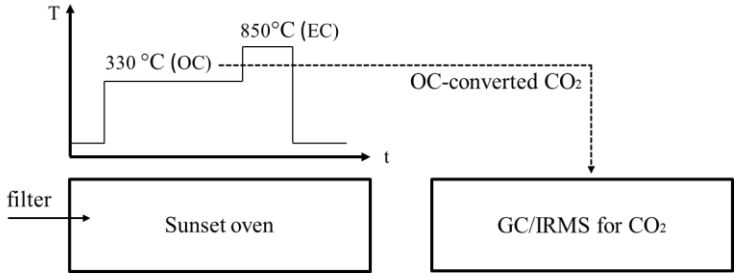

Fig.5. Schematic graph of the set-up for ^{13}C measurement in OC fraction of carbonaceous aerosol, consisting of an oven where aerosol samples are burned in the step temperature scheme shown above and where the weight of OC and EC is measured, a GC/IRMS system where OC-converted CO_2 is then measured for $\delta^{13}C$ revealing $\delta^{13}C$ in OC.

3.4.3 Proton-transfer-reaction mass spectrometry

Proton transfer reaction mass spectrometry (PTR-MS) is an analytical chemistry technique that is most widely used for measuring mixing ratio of VOCs in the atmosphere. The method is based on proton transfer reaction between molecules and hydronium ions (H_3O^+) as is shown in (R1).

$$H_3O^+ + VOC \leftrightarrow VOC \cdot H^+ + H_2O \qquad (R1)$$

The instrument used requires air sample with flow rate of approx. 25mL/min and ambient room pressure when it enters the inlet. The concentration of total concentration of VOCs

in samples must not exceed around 10 ppm. Samples were diluted with zero air to the concentrations in the measurable range.

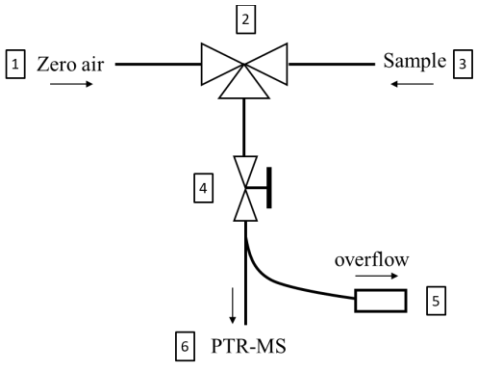

Fig.6. Schematic graph of the set-up for VOC measurement for air samples in the flasks consist of 1) zero air inlet for blanks in between sample measurements, 2) 3-port valve that can be switched between zero air and sample into the gas bench, 3) sample inlet, 4) needle valve to control the flow rate to the gas bench, 5) overflow to ensure ambient pressure of the gas, at which the PTR-MS works. At the end of the overflow, the flow rate is monitored, 6) the inlet of PTR-MS.

3.5 Experiments

In the first stage, I burned fine fuels of willow wood chips (C3), corn silk (C4) and the 1:1 mixture of the two above under the controlled fire set-up. Each fire lasted approx. 10 minutes. In total, there were 13 fires, in which 6 were C3 burnings and C3 and C4 1:1 mixture burning respectively, 1 was C4 burning. Two of the C3 burnings were fueled by willow chips with added moisture by spraying water on the dry wood chips. Such preliminary experiments were meant to see if there were indeed effects of moisture contents on emissions. For each fire, simultaneous air and particle sampling were throughout the whole process of the fire. As a result, air and particle samples here represent the average emission of the whole combustion process from ignition until the end of the fire.

In the second stage, Prunus avium (cherry) wood chunks were used to study the evolution of carbon emission with two fires both lasting approx. 30 minutes. Fuel moisture contents were 12% and 24% respectively. This set was conducted outdoors in no-rain, low-wind condition in an aluminum plate. Samples were directly collected by flask approx. 10 cm

above the fire with dryer and 7-micron filter. The samples in this set were expected to be much concentrated than that of the other two sets, due to less mixing with ambient air compared to the method chamber experiments with pump.

The third stage were conducted in the fire chamber again with cherry wood. There were nine fires, each of which lasted approx. 30 minutes. The moisture contents of the fuel for each fire varied from undetectable to 24%. Instead of taking the average of a fire as in the first set, every fire was sampled twice. Due to sudden unexpected issues with the 20L sample bag, smaller sample bags were used that resulted in duration of samplings to be around 170s rather than covering the whole flaming or smoldering processes as originally planned. Therefore, for each fire one sampling was in the very beginning of the fire, which represented the flaming phase of the fire, the other was in the end of a fire when the fire was in the smoldering phase.

Table 3

Summary of the three sets of experiments

Set	Fuel	Number of samples	Variable(s)	location
wet/dry fuel sequences	willow chips, corn silk	6 (C3) +1(C4) +6(C3+C4)	C3/C4, moisture	fire chamber
AMS: fire	prunus avium chunks	8+8(moisture)	time, moisture	outdoor
AMS: phase	prunus avium chunks	18	moisture	fire chamber

3.6 Data analysis techniques

3.6.1 Keeling plot

Biomass burning species are also abundant at different levels in the background atmosphere. To derive the isotopic composition of CO and CO_2 emitted solely from burning, the Keeling plot analysis (Keeling, 1958) was adopted. It assumes that the concentration of species of interest is the linear sum of the contribution from burning emission and that of the background air. The isotopic composition of the emission source follows

$$\delta_{meas} = \delta_{source} + \frac{1}{C_{meas}} \cdot \frac{C_{bg}}{\delta_{bg} - \delta_{source}} \quad (2)$$

Where c represents concentration and meas, source, bg represents measured, emission source, background levels respectively. With reciprocal of the measured concentration as the x-axis and measured delta value as the y-axis, the y-intercept represents delta value of the source.

3.6.2 Emission ratio

The concepts of emission ratio are often used for studying biomass burning emissions and their correlations. Emission ratio is defined as the ratio between the emission species of interest to a reference gas, for which CO is most commonly chosen owing to its abundance high in burning emissions but low in the background atmosphere (Andreae, 2019). The most common definition for emission ratio (normalized excess mixing ratio) is expressed as (Akagi et al., 2011)

$$NEMR_{X,CO} = \frac{[X]_{sample} - [X]_{bg}}{[CO]_{sample} - [CO]_{bg}} \quad (3)$$

Another common concept is emission factor, which is ratio of the mass of emission and the mass of dry fuel. Compared to emission factor, the advantage of using emission ratio here is that emission ratio is independent of the mass of the fuel burned and does not need the total amount of emission to calculate. The interest of this study is the relative emission species with respect to other emission species.

3.6.3 Modified combustion efficiency

Combustion efficiency of fires varies, depending on the specific fuel, meteorological condition, moisture content of the fuel and so on. A good way to quantify the completeness of a combustion process is modified combustion efficiency (MCE). MCE is defined as the portion of CO_2, the end-product of combustion in the total carbon emission, here approximated by the sum of CO and CO_2 emissions. In such way, MCE can be expressed as

$$MCE = \frac{\Delta CO_2}{\Delta CO_2 + \Delta CO} \quad (4)$$

In which Δ means the enhancement concentration, that is the concentration in the sample minus the concentration of the background level. MCE for natural fires varies from 80% to 94%, in which tropical forest has an average MCE of 91±3% (Andreae et al., 2019).

4. Results

4.1 CO and CO_2 isotopes

First, samples from laboratory plant burning and from Amazon fight campaign were gathered to show the isotopic compositions of CO (Fig. 7 left) with a large spread in both $\delta^{13}C$ and $\delta^{18}O$. For C3 plants, CO isotopes ranged from -10.6 to -35.0 ‰ VPBD in $\delta^{13}C$ and 7.5 to 34.4 ‰ VSMOW in $\delta^{18}O$. From the wood chip (C3) and corn silk (S4) mixture burning, the derived $\delta^{13}C$ and $\delta^{18}O$ in CO from C4 burning ranged from -18.6 to -13.8 ‰ VPBD in $\delta^{13}C$ and 17.8 to 25.5 ‰ VSMOW in $\delta^{18}O$ (Fig. 7 left, purple cross).

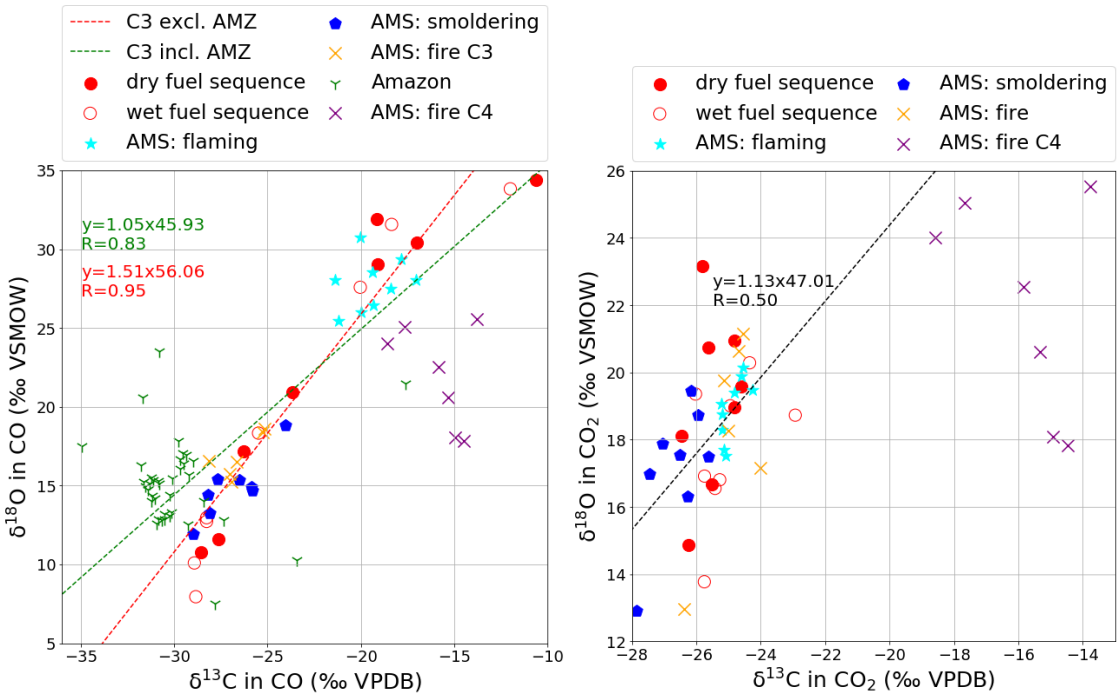

Fig.7. The results for $\delta^{18}O$ plotted against $\delta^{13}C$ in CO (left) and CO_2 (right). Solid and hollow red dots represent long fire sequence with dryer fuel (12%) and with wetter fuel (24%) respectively. Cyan stars and blue pentagons represent 150s-integrated of the flaming and smoldering phase samples respectively, of fires of varying fuel moisture. Orange crosses represent 10min integrated wood chip (C3). Green 'Y' shapes represent Amazon samples. Purple crosses represent 10min integrated corn silk (C4).

Large variation was observed in both $\delta^{13}C$ and $\delta^{18}O$ in laboratory experiments. However, strong positive correlation between $\delta^{13}C$ and $\delta^{18}O$ was also found with correlation coefficient R of 0.95 (Fig. 7 left, red dashed line). Two relatively well-defined groups were found in CO isotopes (Table 4). One was heavier in both carbon and oxygen with $\delta^{13}C$ and $\delta^{18}O$ of -18.2±3.0‰ VPBD and 29.3±2.6‰ VSMOW. Another group was lighter with $\delta^{13}C$ and $\delta^{18}O$ of -27.0±1.6‰ VPBD and 14.9±3.2‰ VSMOW. From the wood chip (C3) and corn silk (S4) mixture burning, the derived $\delta^{13}C$ and $\delta^{18}O$ in CO emission from C4 plants were -15.9±1.9‰ VPBD and 22.2±3.4‰ VSMOW respectively.

Table 4

Two groups observed in CO and CO_2 isotopes. The units of mean values were ‰ vs VPDB for $\delta^{13}C$ and ‰ vs VSMOW for ^{18}O. P-values were obtained through Student's T-test. A p-value of 5% means the hypothesis that the two groups have equal means is rejected at 95% confidence level.

Parameter	Mean (lighter)	Mean (heavier)	p-value (%)
$\delta^{13}C$ in CO	-18.18 ± 1.58	-26.97 ± 0.68	< 1
$\delta^{18}O$ in CO	29.31 ± 1.41	14.89 ± 1.37	< 1
$\delta^{13}C$ in CO_2	-24.77 ± 0.36	-25.81 ± 0.38	< 1
$\delta^{18}O$ in CO_2	19.33 ± 0.73	17.59 ± 0.99	5.3

For Amazon samples, $\delta^{13}C$ and $\delta^{18}O$ were found to be -29.9±2.7‰ VPBD and 15.1±2.9‰ VSMOW, which were close to the lighter group but on average 2.9‰ and 0.2‰ depleted in $\delta^{13}C$ and $\delta^{18}O$ respectively. Except 6 outliners, CO isotopes in most Amazon samples varied in a smaller range with -30.3±1.0‰ VPBD and 14.8±1.5‰ VSMOW.

Similar to CO, samples from laboratory C3 plant burning and from Amazon fight campaign were gathered to show the isotopic compositions of CO_2 (Fig. 7 right). The spread shown in isotopes in CO was smaller than that of CO, with $\delta^{13}C$ and $\delta^{18}O$ of -25.4±0.9‰ VPBD and 18.3±2.1‰ VSMOW respectively. A weak to moderate correlation was also found between $\delta^{13}C$ and $\delta^{18}O$, with correlation coefficient R to be 0.50. The derived $\delta^{13}C$ and

$\delta^{18}O$ in CO_2 emission from C4 plants were -10.0±0.8‰ VPBD and 19.7±2.7‰ VSMOW, dinstict from that of C3 plants.

4.2 Carbonaceous aerosol

Here data from phase average samples (flaming and smoldering) and fire average samples (C3, C4 and C3+C4 mixture) were gathered, in which *AMS: phase* samples provided OC/EC mass concentration and OC $\delta^{13}C$ data while *AMS: fire* samples only had OC $\delta^{13}C$ data. Aerosol data for some samples could not be obtained because of mass concentration lower than the instrument range. Available results from *AMS: phase* show that during flaming, OC emission ratios relative to CO and CO_2 were $(2.7 \pm 1.0) \times 10^{-4}$ $\mu g/(cm^2 \cdot ppb)$ and $(6.6 \pm 8.4) \times 10^{-3}$ $\mu g/(cm^2 \cdot ppm)$, and that during smoldering, OC emission ratios relative to CO and CO_2 were $(4.2 \pm 2.8) \times 10^{-5}$ $\mu g/(cm^2 \cdot ppb)$ and $(3.7 \pm 2.0) \times 10^{-3}$ $\mu g/(cm^2 \cdot ppb)$. OC/TC mass concentration during flaming and smoldering phase were 75±23% and 88±12%.

For OC mass concentration in flaming phase, a positive correlation with CO mixing ratio and a moderate negative correlation with CO_2 mixing ratio were observed (Fig. 9), with correlation coefficient R of 0.83 and -0.74, respectively. For OC mass concentration during smoldering phase, however, the spread was too large to see any correlation. EC fraction did not show any clear correlation with either CO or CO_2 mixing ratios in emissions.

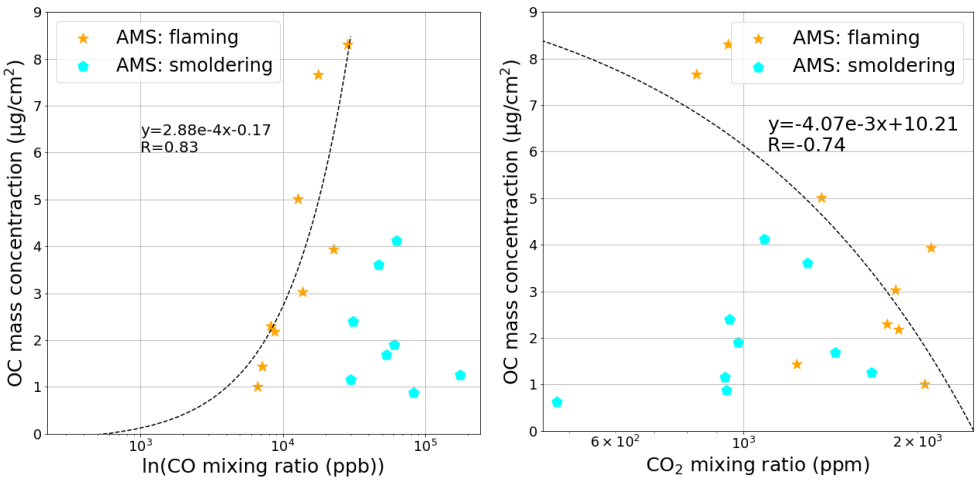

Fig.9. The results for CO (left) and CO_2 (right) mixing ratios in samples plotted against OC mass concentration. Orange stars and cyan pentagons represent 150s-integrated of the flaming and smoldering phase samples, respectively.

Except for flaming samples, $\delta^{13}C$ in CO correlates well with that of OC, with correlation coefficient $R^2 = 0.90$ (Fig. 11 left). For flaming average samples, $\delta^{13}C$ in OC is depleted compared to that of CO by 5.5±2.3 ‰. Correlation of $\delta^{13}C$ in OC and in CO_2 is also observed, which is however weaker than the correlation of $\delta^{13}C$ in OC and in CO excluding flaming phase samples, with correlation coefficient $R^2 = 0.67$ (Fig. 11 right). The correlation is weak with wood chip and corn silk mixture fuel burnings where $\delta^{13}C$ in CO_2 is rather constant at around -17.8±0.2 ‰, $\delta^{13}C$ in CO_2 varies up to 1.4‰. $\delta^{13}C$ in CO_2 for C4 (corn silk) fire average is not available here since CO_2 enrichment in the sample is too low compared to the background. However, the fuel content ^{13}C measurement shows $\delta^{13}C$ of -12.61‰, which is 2.6‰ enriched in ^{13}C relative to OC.

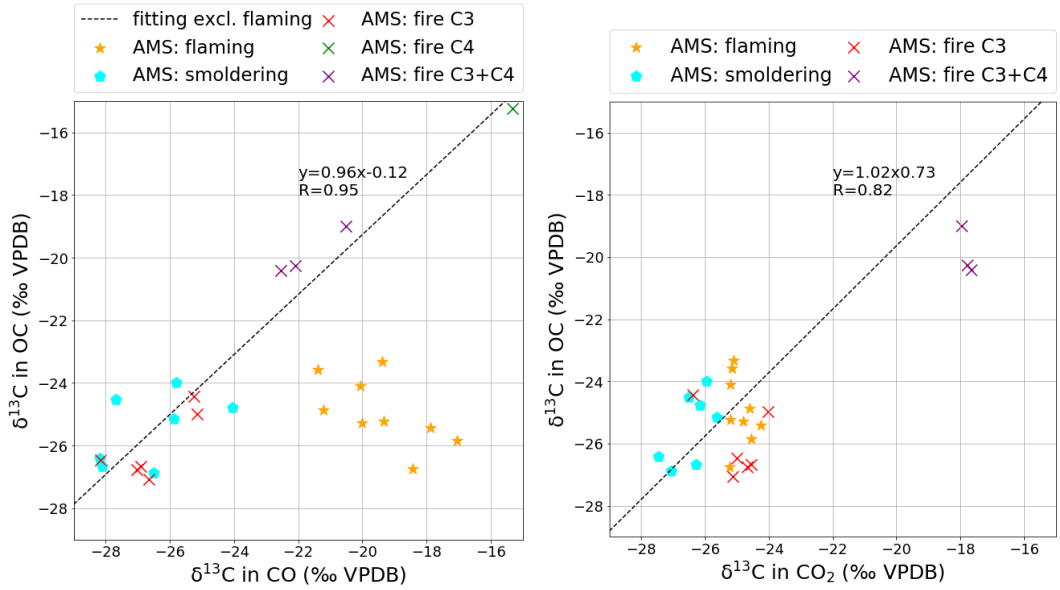

Fig.11. The results for $\delta^{13}C$ in organic carbon $\delta^{13}C$ fraction in carbonaceous aerosol plotted against $\delta^{13}C$ in CO (left) and CO_2 (right). Orange stars and cyan pentagons represent 150s-integrated of the flaming and smoldering phase samples, respectively. Red and purple crosses represent 10min integrated wood chip (C3) and wood chip (C3)+ corn silk (C4) mixture, respectively.

4.3 Evolution in emissions of fire

In this section, long fire experiment samples, in total, 16 samples were gathered to show the evolution of fire emissions. Within the time period of combustion, MCE showed overall decreasing trend for both dry fuel (12% of water) and wet fuel (24% of water), starting from near complete combustion (MCE higher than 99%) to as low as 68%. The trend in MCE, however, showed considerable amount of noise, especially for wet fuel emission (Fig. 12). By visual observation of the appearance of the fire, the first three samples were taken in the flaming phase for both fuels. The last three and the last four samples were taken in the smoldering phase for dry and wet fuel respectively. However, the distinctive features of burning phase was not visible in MCE values. MCE in two different fuels, dry fuel and wet fuel did not show significant difference (with p-value of 61% in Student's T-test).

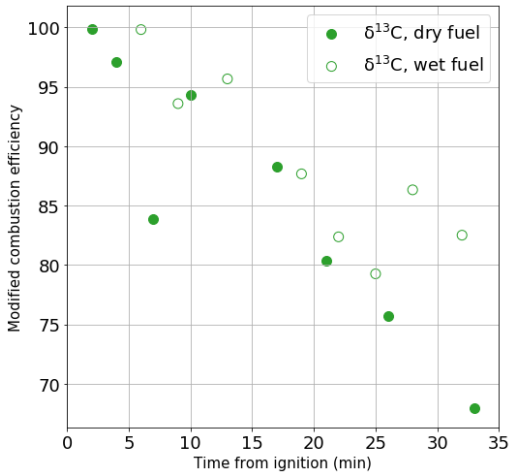

Fig.12. The results for modified combustion efficiency (%) plotted against time from ignition (min). Solid dots represent dry fuel burning and hollow dots represent wet fuel burning.

The variation in $\delta^{13}C$ and $\delta^{18}O$ in CO throughout the fire process showed strong decreasing trend over time from ignition (Fig. 13, left). The difference in $\delta^{13}C$ and $\delta^{18}O$ between flaming and smoldering samples were up to -17.9‰ VPDB and -21.1‰ VSMOW respectively. Indication of burning phases could be seen in isotopes of CO. Both $\delta^{13}C$ and $\delta^{18}O$ experienced relatively stable periods towards the beginning and the end, which

roughly but not exactly coincided with observation of the visual characteristics of burning behaviors.

Compared to CO, CO_2 experienced little isotopic fractionation. $\delta^{13}C$ and $\delta^{18}O$ from burnings could be characterized as -25±0.8‰ VPDB and 18±2.3‰ VSMOW. Decreasing trend in the secondary isotopes, although weaker than in CO, was also shown. The difference in $\delta^{13}C$ and $\delta^{18}O$ between flaming and smoldering samples were up to -1.6‰ VPDB and -8.3‰ VSMOW. No indication of burning phases was observed in isotopes of CO_2.

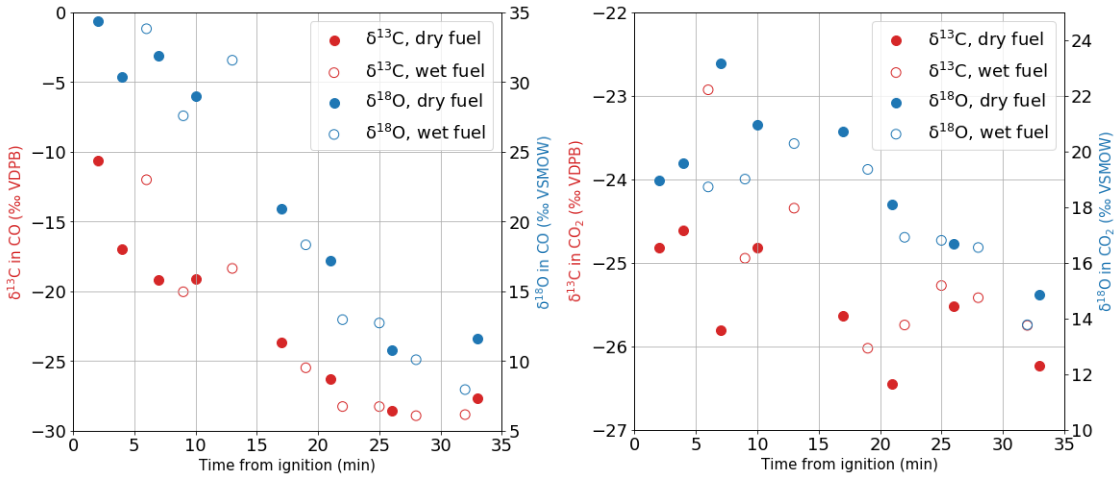

Fig.13. The results for $\delta^{13}C$ and $\delta^{18}O$ in CO (left) and CO_2 (right) emission from two long fire experiments with dry wood (12% of water, solid dots) and wet wood (24% of water, hollow dots). The results are plotted against the time from ignition.

Assuming constant mixing ratio with background air for all samples, mean CO emission isotopes could be derived from CO mixing ratios and its isotopic ratios in all samples. In such a way, a rough estimate of the mean $\delta^{13}C$ and $\delta^{18}O$ in CO from burning emission were -26.9‰ VPDB and 14.1‰ VSMOW.

No significant difference in CO and CO_2 isotopes was found between dry fuel and wet fuel, despite relatively large difference in moisture contents of the fuels (Table 5). More about the effect of moisture are presented in Section 4.5.

Table 5

CO and CO_2 isotopes emitted from dry and wet fuel. The units of mean values are ‰ vs VPDB for $\delta^{13}C$ and ‰ vs VSMOW for ^{18}O. P-values are obtained through Student's T-test. A p-value of 5% means the hypothesis that the two groups have equal means is rejected at 95% confidence level.

Parameter	Mean (dry fuel)	Mean (wet fuel)	p-value (%)
$\delta^{13}C$ in CO	−22.2 ± 4.7	−24.1 ± 4.6	51
$\delta^{18}O$ in CO	22.0 ± 7.4	18.4 ± 7.7	44
$\delta^{13}C$ in CO_2	−25.5 ± 0.6	−25.1 ± 0.8	33
$\delta^{18}O$ in CO_2	19.1 ± 2.2	17.7 ± 1.7	24

VOCs were observed to be mostly emitted during early phase of emission by investigating the emission ratio of VOCs to CO_2. However, for HCN and acetonitrile, VOC emission ratio to CO_2 increased near the end of the combustion process. The effect of fuel moisture was not clear from the data due to rather large variability in VOC emission ratios from both fuels.

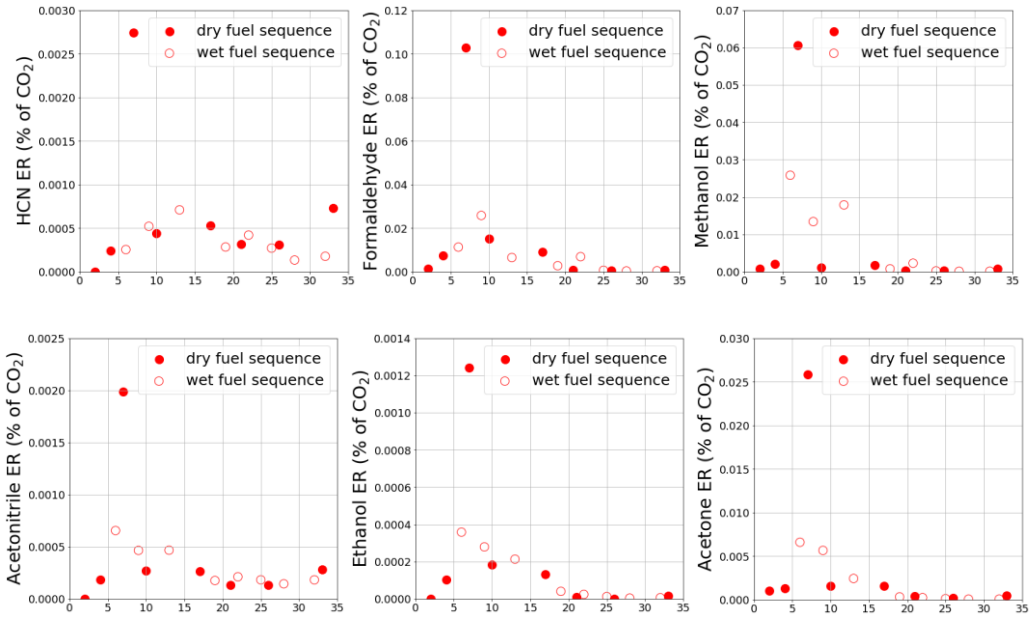

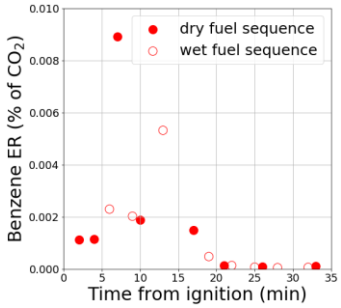

Fig.14. The results for VOC emission ratios to CO_2 (% of CO_2) plotted against time from ignition.

Due to the limited number of datapoints, the results here were not enough to indicate any influence of fuel moisture on MCE and isotopes in CO and CO_2 emission over the combustion process.

4.4 Combustion efficiency and emissions

Here all the data for C3 plants burnings were combined to show the effect of combustion efficeincy on CO and CO_2. The data included were 2 long fire experiment sequences with 16 samples in total, 9 samples of flaming phase and smoldering phase each, and 6 samples of wood chip burnings. The range of MCE of all samples was between 68% to nearly 100% (Table 6). $\delta^{13}C$ and $\delta^{18}O$ were plotted against MCE for both CO and CO_2, as is shown in Fig. 14 (left).

Table 6

Modified combustion efficiency among samples

Sample type	MCE (%)
AMS: Flaming phase	96.3±4.2
AMS: Smoldering phase	87.0±6.1
Long fire sequences	87.2±9.1
AMS: Wood chip fire	96.1±1.9

A strong positive correlation was observed between CO isotopic ratios and MCE. The more efficient the combustion was, the heavier the emitted CO was in terms of both carbon (Fig. 14a) and oxygen(Fig. 14c). When MCE was below around 80% to 90%, $\delta^{13}C$ and $\delta^{18}O$ in CO remained relatively constant before an sharp increase with increasing MCE. $\delta^{13}C$ in

CO reached at the highest value, around -11 ‰ to -12 ‰ when the MCE was above 99.8%. $\delta^{18}O$ followed similar trend with maxium value around 35‰. The variation in $\delta^{18}O$ within the trend, however, was rather large compared to $\delta^{13}C$. From the data obtained, it ranged from 8‰ to 34‰. A non-linear empirical equation (an adaption of Steinhart and Hart Equation) was created to fit the pattern of $\delta^{13}C$ and $\delta^{18}O$ in CO against MCE (Fig. 14a, c).

A weak to moderate correlation was observed between the isotopic ratios in CO_2 and MCE. Compared to CO, $\delta^{13}C$ and $\delta^{18}O$ was rather constant throughout all combustion efficiency levels. A increasing trend, however, was still significant both between $\delta^{13}C$ and MCE and between $\delta^{18}O$ and MCE in CO_2. $\delta^{13}C$ covered the range of -28 to -23‰ while $\delta^{18}O$ 13 to 23‰. (Fig. 14c,d)

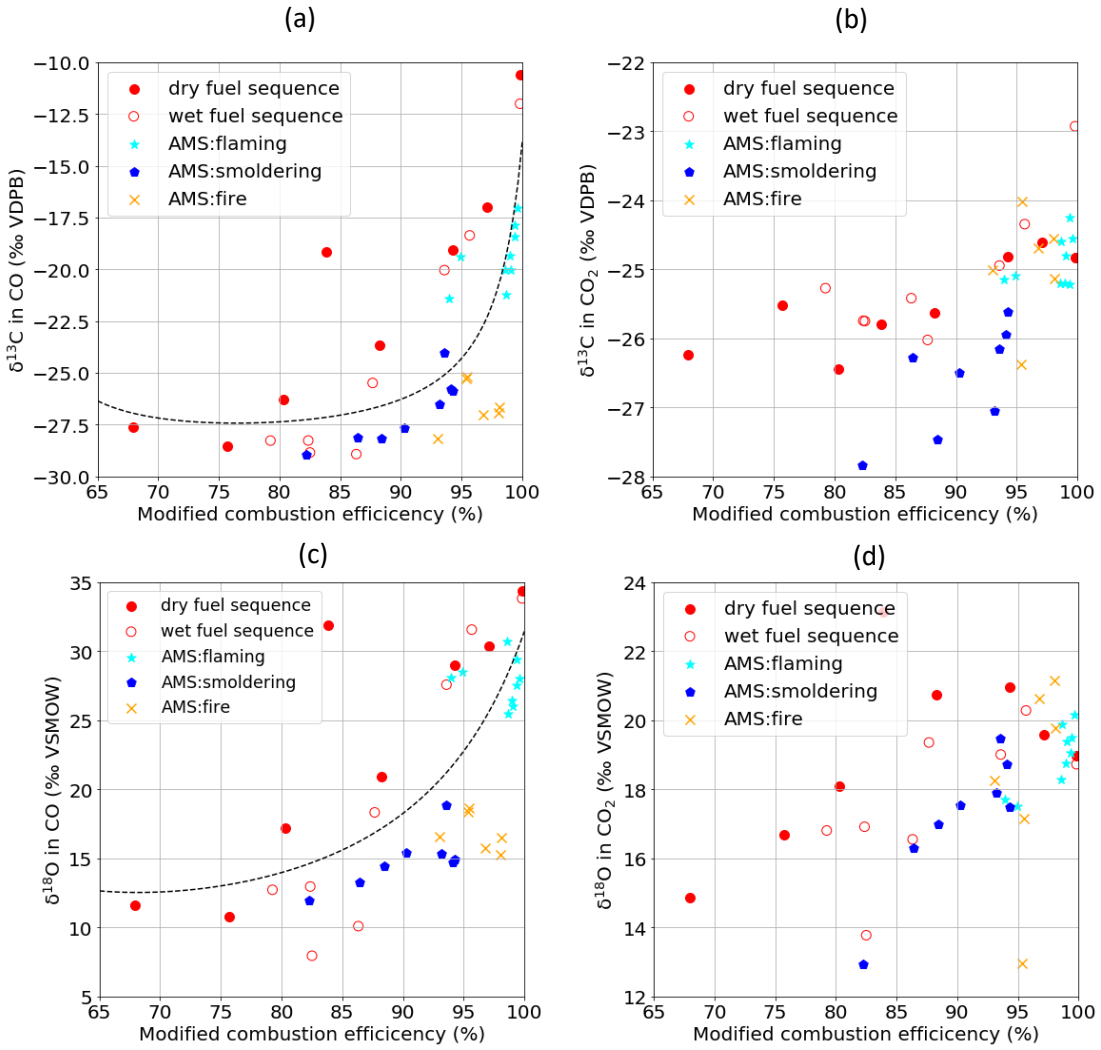

Fig.14. The results for $\delta^{13}C$ (a, c) and $\delta^{18}O$ (b, d) in CO (a, b), CO_2 (c, d) plotted against modified combustion efficiency. Solid and hollow red dots represent long fire sequence with dryer fuel (12%) and with wetter fuel (24%) respectively. Cyan stars and blue pentagons represent 150s-integrated of the flaming and smoldering phase samples, respectively. Yellow crosses represent 10min integrated wood chip (C3) burning. The expression for the fitting is $\delta = (a + b \cdot \ln(\delta) + c \cdot \ln(\delta)^2)^{-1} + d$. For $\delta^{13}C$ a=-55.01, b=19.16, c=-0.3398, d=30. For $\delta^{13}C$ a=-3.689, b=1.339, c=-0.02504, d=0.

For carbonaceous aerosols, the results showed that in more complete combustion,OC fraction was more dominant in carbonaceous aerosols. However large spread was also observed. For flaming phase samples only, a sharp decrease in OC was observed along with increase in combustion efficiency (Fig. 15 left). Within flaming and smolderin phase groups, higher combustion efficency was linked to lower OC/TC ratio. In flaming samples, decrease in $\delta^{13}C$ in OC was observed with increasing modified combustion efficiciency with correlation coefficent R=-0.82 (Fig. 15 right).

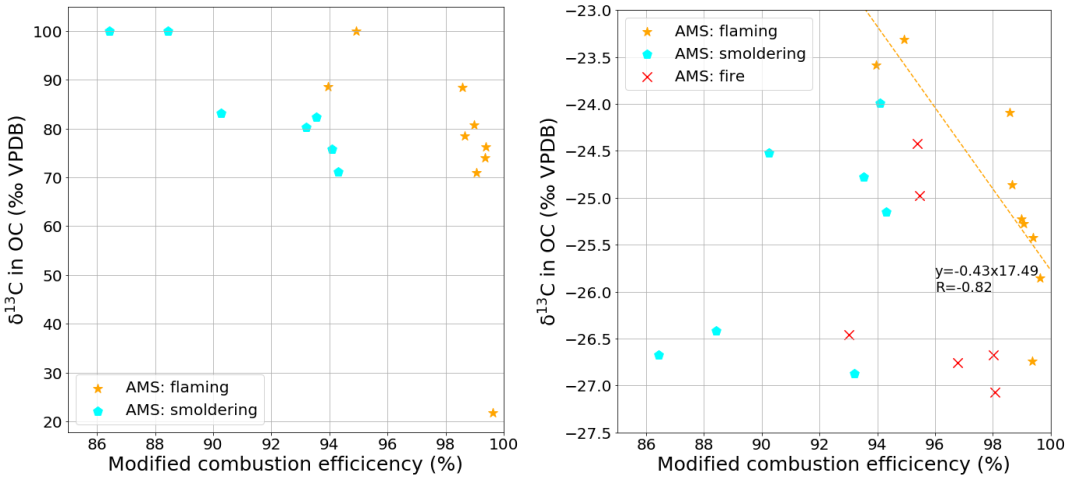

Fig.15. The results for mass concentration of OC (without black frame) and EC fractions (with black frame) in carbonaceous aerosol plotted against modified combustion efficiency. Orange stars and cyan pentagons represent 150s-integrated of the flaming and smoldering phase samples, respectively. Red crosses represent 10min integrated wood chip (C3) burning.

4.5 Burning phases and emissions

In total, there were 13 samples representing flaming and smoldering phases of fire respecitively. All samples from 150s phase average emission were used in this section. Moreover, the 2nd and 3rd samples from long fire experiments were chosen to represent flaming phase while the 6th and 7th samples from long fire experiments were chosen to

represent smoldering phase. Such selection was meant to compare samples here with that of 150s phase average samples. From the samples selected, the flaming phase was characterized by MCE of 96.3±4.2% whereas smoldering MCE of 87.0±6.1% (Table 7).

Despite large spread within one burning phase, well-defined burning phases were observed in CO isotopic ratios with no overlapping of isotopic signatures between phases in terms of either carbon or oxygen (Fig. 16 ,left). On average in CO emission, ^{13}C was depleted by 8.1‰ and ^{18}O was depleted by 14.5‰ in smoldering relative to flaming. During flaming phase, $\delta^{13}C$ ranged from -21.4‰ to -27.6‰ and $\delta^{18}O$ from 25.5‰ to 31.9‰. During smoldering phase, $\delta^{13}C$ ranged from -28.9‰ to -24.9‰ and $\delta^{18}O$ from 8.0‰ to 18.8‰ (Table 7).

Table 7

Characteristic isotopic composition of CO and CO_2 in flaming and smoldering phases. The mean and standard deviation are derived from the samples. Units are ‰ vs VPDB for $\delta^{13}C$ and ‰ vs VSMOW for ^{18}O.

Phase	flaming	smoldering	p-value (%)
MCE (%)	96.3±4.2	87.0±6.1	1.1
$\delta^{13}C$ in CO	-19.2±1.3	-27.3±1.5	< 1
$\delta^{18}O$ in CO	28.6±2.0	14.1±2.4	< 1
$\delta^{13}C$ in CO_2	-24.9 ±0.4	-26.3±0.8	< 1
$\delta^{18}O$ in CO_2	19.4±1.4	17.1±1.6	4.6

As for CO_2 emission, distinct isotopic signatures for two different phases were also found, however with overlaps in the values of $\delta^{13}C$ and $\delta^{18}O$ (Fig. 16 ,right). During smoldering phase, $\delta^{13}C$ ranged from -27.8‰ to -25.4‰ and $\delta^{18}O$ from 8.0‰ to 19.5‰. During flaming phase, $\delta^{13}C$ ranged from -25.2‰ to -24.3‰ and $\delta^{18}O$ from 8.0‰ to 31.9‰. It was still possible to distinguish flaming and smoldering by looking at both carbon and oxygen isotopes in CO_2. As is shown in Fig. 16 (right), a clear line could be drawn between two phases when $\delta^{18}O$ was plotted against $\delta^{13}C$. On average in CO_2 emission, $\delta^{13}C$ and $\delta^{18}O$

were depleted in the same way as in CO, but on different magnitude. In CO_2, $\delta^{13}C$ was depleted by 1.4‰ and $\delta^{18}O$ was depleted by 2.3‰ in smoldering relative to flaming, which were smaller compared to that of CO.

For both CO and CO_2, the spread in isotopic ratios was larger for $\delta^{18}O$ than for $\delta^{13}C$, for smoldering than for flaming (Fig 16 and Table 7).

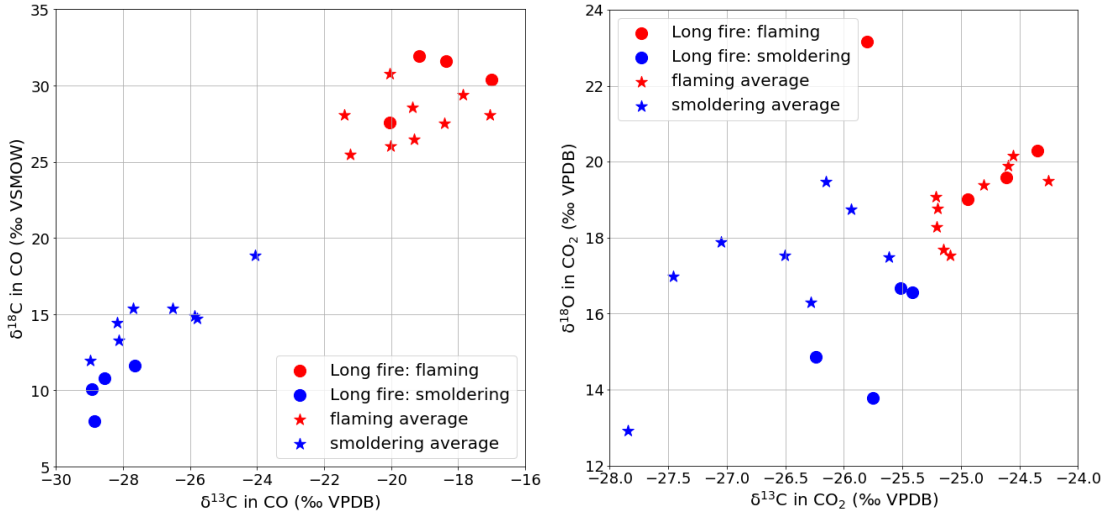

Fig.16. The results for $\delta^{13}C$ (x axis) and $\delta^{18}O$ in CO (left) and CO_2 (right) emission, divided by burning phases: red and blue represents flaming and smoldering phases, respectively. Dots represent samples from long fire sequence and stars represent samples from phase experiments.

No distinct features for flaming and smoldering phases were found regarding OC fraction of carbonaceous aerosol and VOC emissions.

4.6 Fuel moisture and emissions

Preliminary results showed enrichment of $\delta^{13}C$ in both CO and OC fraction of carbonaceous aerosol in two fire emissions of moisturised wood chip fuel. Here, all the available results with known fuel moisture content were gathered to show the effect of fuel moisture content on emission. Possible fuel moisture content in this study were 0, 2, 4, 7, 10, 17, 21, 23 (for two fires) and 26%. For each fuel burning, one sample for flaming and one sample for smoldering were taken with nine fires in total and thus 18 samples were used in this section. $\delta^{13}C$ was missing in CO, CO_2 and/or OC for several samples because of low amount. During experiments, it took significantly longer time to ignite fuel with

higher moisture content. In the extreme case of fuel with moisture content of 23, it took around 8min to ignite the fuel. However, after ignition, the burning process by visual observation were not significantly influenced by different fuel moisture levels, in terms of duration of either the whole fire, flaming or smoldering.

Surprisingly, no correlation between fuel moisture and MCE were found. In general, correlations between isotopes and moisture content were rather weak (Fig. 17). For flaming phase samples Significant negative correlations were found between $\delta^{13}C$ in CO and fuel moisture content (Fig. 17 a) and between $\delta^{18}O$ in CO_2 and fuel moisture content (Fig. 17 e). Smoldreing phase samples did not show signficant trends.

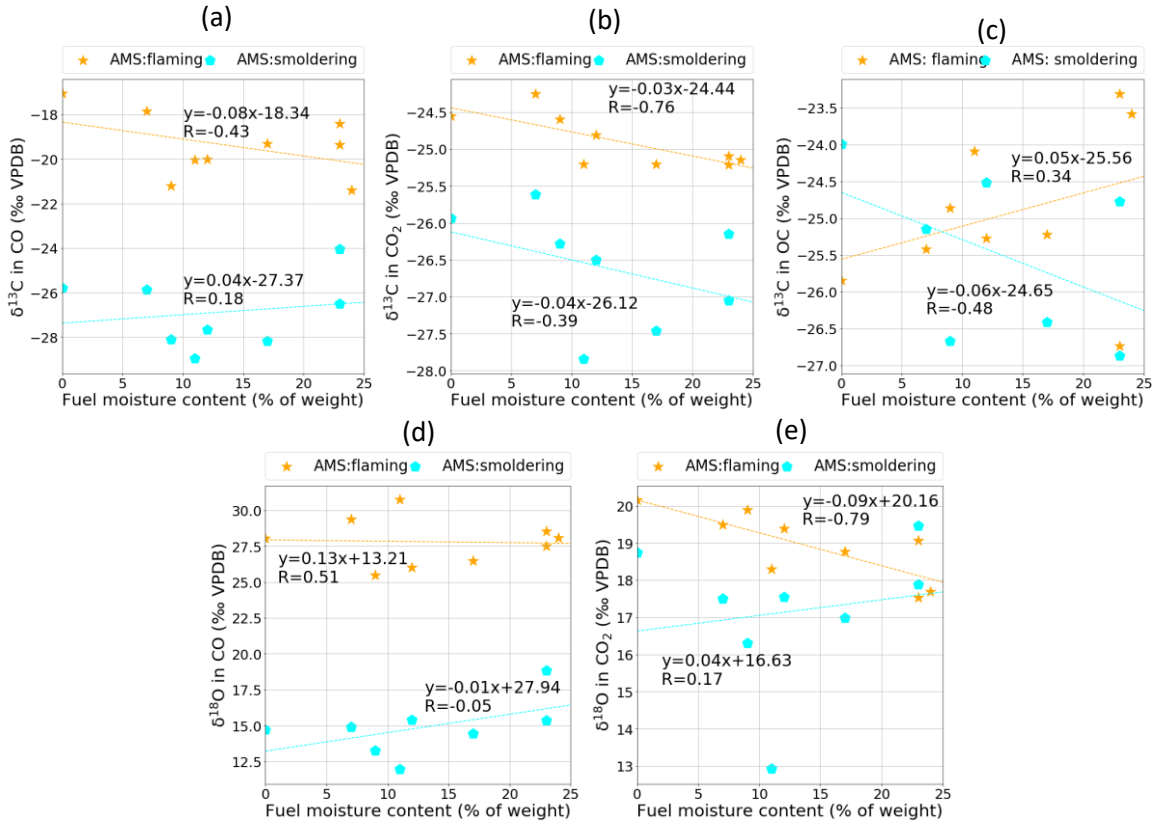

Fig.17. The results for $\delta^{13}C$ and $\delta^{18}O$ in CO (a, d), CO_2 (b, e) and $\delta^{13}C$ (c) in OC fraction emission plotted against fuel moisture content. Orange stars and cyan pentagons represent 150s-integrated of the flaming and smoldering phase samples, respectively.

A significant positive correlation between OC/TC ratio and fuel moisture content was found in the results. With higher fuel moisture, OC fraction tended to be more dominant in total carbonaceus aerosols.

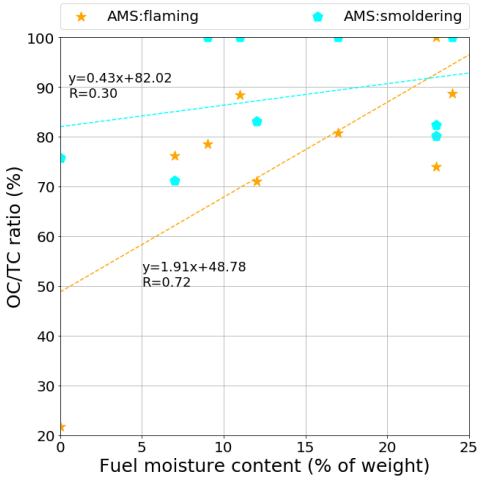

Fig.18. The results for OC/TC ratio (%) plotted against fuel moisture content. Orange stars and cyan pentagons represent 150s-integrated of the flaming and smoldering phase samples, respectively. Red crosses represent 10min integrated wood chip (C3) burning.

4.7 VOC emissions

Results suggested huge spread in VOC emissions and as is shown in Section 4.2, VOCs were mostly emitted in a certain period of time during a combustion process. Mean values in the results together values for savanna and tropical forest burnings (Andreae, 2019) for VOC emission are shown in Table 8. The mean values from laboratory experiments were not comparable to the typical values for savanna and tropical forest burnings.

Table 8

The range of values for VOC emission ratios to CO_2 from results of this study and of derived emission ratio from emission factor in Andreae, 2019 (*) for typical savanna and tropical forest burnings. Units are % of CO_2.

Type	acetonitrile	acetone	HCN	formaldehyde	acetaldehyde

Amazon campaign	0.00028 - 0.37	0.0044 - 0.012	0	0.00021 - 0.0043	0.0010 – 0.0076
AMS: fire	0.00020 – 0.010	0.003 – 0.61	0.00029 – 0.048	0.020 – 0.30	0.00047 – 0.049
AMS: flaming	0 - 0.0027	0.00014 - 0.0044	0.000049 - 0.0056	0.0096 - 0.35	0.00024 - 0.018
AMS: smoldering	0 - 0.0031	0 - 0.0043	0 - 0.041	0 - 0.13	0 - 0.0075
Fire sequence	0 – 0.0020	0.000060 – 0.026	0 - 0.0027	0.00032 - 0.10	0.000049 - 0.0089
Savanna*	0.010	0.028	0.027	0.074	0.051
Tropical forest*	0.030	0.039	0.027	0.148	0.140

5. Discussion

5.1 CO isotopes

Including all samples from C3 plants controlled burning, $\delta^{13}C$ and $\delta^{18}O$ in CO emission can be characterized as -23.4±4.8‰ VPBD and 20.8±7.7‰ VSMOW (Table 9). From Fig. 7, two isotopically different groups were observed, which largely correspond to flaming and smoldering phase emissions. The values obtained here is close to the known chacteristic isotopic composition (Röckmann et al., 2002) of CO with $\delta^{13}C$ and $\delta^{18}O$ as -22.9‰ VPBD and 17.2‰ VSMOW respectively, which are 0.5‰ VPBD in $\delta^{13}C$ and 3.6‰ VSMOW in $\delta^{18}O$ more enriched in secondary isotope than the mean values of this study. Samples that represented emission from the whole combustuin process lie in the group of smolering phase CO, confirming that average isotopic ratio of CO during a whole combustion process should be close to that of the smoldering phase emitted CO.

For Amazon forest fire samples, $\delta^{13}C$ and $\delta^{18}O$ are found to be -29.9±2.7‰ VPBD and 15.1±2.9‰ VSMOW, which are depleted in ^{13}C and ^{18}O relative to the known characteristic values by 7‰ VPBD and 2.1‰ VSMOW respectively. Interestingly, Amazon samples lie closely together with samples that presumably correspond to the C3 plant smoldering phase emission but with lower $\delta^{13}C$ and higher $\delta^{18}O$.

The derived $\delta^{13}C$ and $\delta^{18}O$ in CO from C4 plants can be chacterized as -15.9±1.9‰ VPBD and 22.18±3.4‰ VSMOW. Results suggest that due to the large range of CO isotopes, flaming phase emitted CO have similar isotopic ratios to that of C4 plants. This suggest it is not always possible to distinguish C3 and C4 burnings by CO isotopes. $\delta^{13}C$ in CO from

C3 in this study lies in the range of -16.5 to -10.2‰ VPBD reported by Kato et al. (1999b), however, CO is enriched in ^{18}O relative to the upper limit of the Kato et al. (1999b)'s range of 3.0 to 16.2‰ VSMOW.

Table 9

Isotopic compositions of CO obtained from controlled C3 plant burning experiments and Amazon forest fire flight campaign in this study and the characteristic values from Röckmann et al. (2002) and model a priori for Forrest burning from Bergamaschi et al., 2000.

Type	Controlled fire (averaged total)	Amazon campaign	Röckmann et al., (2002)	Model a priori (Bergamaschi et al., 2000)
$\delta^{13}C$ in CO	-26.9	-29.9±2.7	-22.9	-25.0+3.0
$\delta^{18}O$ in CO	14.1	15.1±2.9	17.2	10.0±10.0

Few studies have been done in characterizing the isotopic compositions of CO in biomasss burning emission. Kato et al. (1999b) found the dependence of CO isotopes on the burning phase. A trend towards lighter carbon and oxygen over time throughout the combusion process was observed. Kato et al. (1999b) concluded that in CO emission $\delta^{13}C$ is 2.7 to 10.4 ‰ VPBD heavier in flaming phase relative to smoldering phase.

Table 10

Isotopic compositions of CO in flaming and smoldering phases of cherry wood trunk (C3) in this study and Eucalyptus branches (C3) in Kato's study (shown in brackets). F - S represents the difference in δ values between flaming and smoldering phases.

Phase	Controlled fire	Flaming	Smoldering	F - S
MCE (%)	91.7±7.6	96.3±4.2	87.0±6.1	9.3
$\delta^{13}C$ in CO	-23.4±4.8	-19.2±1.3 (-24.0)	-27.3±1.5 (-29.7)	-7.7±1.4 (-5.7)
$\delta^{18}O$ in CO	20.8±7.7	28.6±2.0 (26.0)	14.1±2.4 (18.4)	-12.9±2.8 (-7.5)

By investigating the isotopic compositions of CO for the two phases of fire separately, this study verifies such decreasing trend of $\delta^{13}C$ in CO but indicates stronger isotopic fractionation in producion of CO. The difference between flaming and smoldering in $\delta^{13}C$

is -7.7±1.4 ‰ VPDB and the difference in $\delta^{18}O$ -12.9±2.8‰ VSMOW (Table 10). Assuming the fuel content $\delta^{13}C$ to be 25.5‰ VPDB (derived from average $\delta^{13}C$ in CO_2 emission of the same fuel), the flaming phase emitted CO indicate on average an enrichment of 6.3‰ VPDB in ^{13}C compared to that of the fuel content, well beyond depletion of 0.6 to 3.6‰ VPDB suggested by Kato et al. (1999b). In the smoldering phase, $\delta^{13}C$ in CO indicate on average a depletion of 1.8‰ VPDB compared to that of the fuel content, which however is below Kato et al. (1999b)'s range of 2.1 to 6.8‰ VPDB depletion. This indicates weaker isotopic fractionation in the smoldering phase than previously thought.

This study verified similar trend for $\delta^{18}O$. What was also found and verified is that compared to atmospheric oxygen ($\delta^{18}O \approx 23.5$‰ VSMOW), ^{18}O in CO is 5.1‰ VSMOW enriched in the flaming phase but 9.4‰ VSMOW depleted in the smoldering phase. Oxygen atoms in CO are both from atmospheric oxygen and fuel content. The $\delta^{18}O$ of fuel is partially determined by $\delta^{18}O$ in the surrounding water used by plant growth, with typical value of 26‰ VSMOW. The proportion of oxygen in CO from atmosphere and fuel content remains unclear.

5.2 CO_2 isotopes

Including all samples from C3 plants burning, $\delta^{13}C$ and $\delta^{18}O$ in CO_2 emission can be characterized as -25.4±0.9‰ VPBD and 18.3±2.1‰ VSMOW. The derived $\delta^{13}C$ and $\delta^{18}O$ in CO emission from C4 plants can be chacterized as -10.0±0.9‰ VPBD and 19.7±3.0‰ VSMOW.

Most carbon content of the burning fuel is emitted to the atmosphere in the form of CO_2. Presumably this leaves little room for isotopic fractionation in CO_2 emission. The fuel $\delta^{13}C$ content measurement is based on the fact that in the case of complete combustion, the $\delta^{13}C$ in emitted CO_2 perfectly represents $\delta^{13}C$ ratio of the fuel. Previous studies have usually assumed for simplification no isotopic fractionation in the production of CO_2 from biomass burning. This study verifies that $\delta^{13}C$ in CO_2 emision largely represents $\delta^{13}C$ in fuel. Its value can be used to distinguish C3, C4 burnings and provide a rough estimate of the ratio of C3 and C4 if both types of fuel are present. However, what was also found in this study

is significant variation in CO_2 isotopes during combusition, even with the same fuel. This leads to a trend in $\delta^{13}C$ similar to that of CO, but to a lesser extent. The difference between flaming and smoldering in $\delta^{13}C$ is -1.4‰ VPDB and the in $\delta^{18}O$ 2.3‰ VSMOW. Unlike CO, $\delta^{18}O$ in CO_2 is always lighter relative to that of atmospheric oxygen and the typical $\delta^{18}O$ in fuel content. Such value for $\delta^{18}O$ in CO_2 indicates isotopic fractionation concerning utilizing oxygen from either or both oxygen source(s).

5.3 Carbonaceous aerosol

Carbonaceous aerosols emission from biomass burning are known to have a very high OC/EC ratio and therefore fire emissions may contribute significantly to OC fraction concentrations in the atmosphere but have limited effect on EC fraction concentrations (Pio et al., 2011). By looking at mass concentration of OC and EC, this study confirmed this idea. In some extreme cases, nearly no EC fraction is detected (with mass concentration on filter less than 0.01μg/cm^2). The average OC/TC ratio in this study is 81.8±18.4%. Previous studies have shown large spread in OC/TC ratio ranging from 35 to 97% and fuel moisture content was suspected to be one of the factors (Chen et al., 2010).

Results shows that OC mass concentration is positively correlated with CO concentration, but negatively correlated with CO_2 concentration during flaming phase. This may reconfirm the assumption that OC emission is closely associated with incomplete combustion. However, such correlations were not found among smoldering phase samples. This may be related to the difference in fire behavior between burning phases, which leads to filter sampling biases.

$\delta^{13}C$ in OC and CO shows strong correlation with the notable exception of flaming phase samples. This may again be related to the emission of OC during incomplete combustion. Interestingly, $\delta^{13}C$ of OC in flaming samples and MCE were anti-correlated, as opposed to observed positive correlation between ^{13}C of OC and MCE. The relationship between $\delta^{13}C$ of OC and MCE is still unclear. ^{13}C in OC and CO_2 also shows moderate correlation. With these preliminary results, it is still difficult to draw any conclusion. However, the results imply that isotopic fractionation in the production of OC do not simply follow the same pattern as CO or CO_2.

5.4 Effect of combustion efficiency on emissions

Previous studies indicate the linkage of isotopic compositions of CO to the burning phases or time from ignition when CO is emitted, but not dicrectly to combustion efficiency. In this study, by putting all the samples together with information of CO and CO_2 mixing ratios and isotopes, robust pattern linking $\delta^{13}C$ and $\delta^{18}O$ in CO to modified combusiton efficiency was found. This implies a close relationship between isotopic fractionation of CO and combustion efficiency. An immediate implication is to characterize isotopic compostion of CO according to combustion efficiency, which can either be estimated by typical values of the type of fuel burned, or by calculating from concentrations of CO and CO_2. However, such results are still preliminary.

5.5 Effect of fuel moisture on emissions

The effect of moisture on emissions in Chen et al. (2010) was not reproduced in this study. No enhancement in $PM_{2.5}$ and OC emissions were observed with increasing fuel moisture content. Neither do isotopes in CO, CO_2 and OC show any dependency on fuel moisture. However, it was not certain at what stage the water in the fuel was emitted. It did show during the experiments that wetter fuel took much more time to ignite. This may indicate the possibility that much of the water content might have been emitted during ignition and the most effect from water was thus in the ignition process, which were not sampled. In addition, different time for igniting the fuel may mean that the parameter *time from ignition* were not comparable between fires with fuels of different moisture contents. As is known from Section 4.2 that isotopes in CO and CO_2 evolves over time throughout the combustion process, the effect of fuel moisture on emissions may be much smaller than the effect of uncertainties in the combustion process in some cases.

5.6 Limitations and outlook

Sampling biases is one limitation in this study. As mentioned in Section 3.1.1, in-situ measurement of isotopic composition of CO and CO_2 is not possible. In order to maintain the consistency for analysis, air sampled in the glass flask were used to study fire emission, which brought sampling biases to the results concerning the timing of taking samples. In addition, emission factor cannot be derived without continuous in-situ measurement of emission concentration. The absence of emission factors can be a drawback in the sense

that emission factor is one of the main concerns of studies on biomass burning. As an add-on to the current controlled fire facility, an automated system for air sampling can be built in such a way that there is no interval in between samples and thus eliminating biases.

Treatment of fuel is another limitation of this study. Adding moisture to fuel may not reflect varying moisture content of fuel in nature. During the treating process, the fuel had to undergo a baking process, which might be related to extremely low VOC mixing ratios in the sample. Previous studies have linked $\delta^{13}C$ of fuel to annual precipitation in the environment and indirectly to fuel moisture content. Using fuel with moisture gained naturally in plants may be a more realistic emulation of wildfires.

VOC is known to be chemically active with other biomass burning emission species. It is yet to test whether VOCs are stable in the glass flasks. From the results shown in this study, VOC emission ratios against CO or CO_2 tend to have large spread on several scales of magnitude and they deviate from the average value in the literature. It might be indicative of the importance of in-situ measurement, if possible, for VOC specie in biomass burning.

6. Conclusion

In this study emissions from biomass burning have been investigated using four sets of data. Emissions were studied as a time series in a combustion process from ignition to the end of the fire and were separated by flaming and smoldering phases to study dependency of emissions on burning phases. Both C3 and C4 plants were used as fuels to study the different CO and CO_2 isotopes from emission of burnings of different types of fuel.

This study characterizes isotopic signatures in CO and CO_2 for C3 and C4 burnings with samples from laboratory fire experiments. The study reveals a strong correlation between $\delta^{13}C$ and $\delta^{18}O$ in CO. Isotopic fractionations are found in the production of both CO and CO_2. The strong dependency of $\delta^{13}C$ and $\delta^{18}O$ in CO combustion efficiency and on burning phases are shown in the results. The robust pattern of the dependency of CO isotopes and combustion efficiency may potentially be used to estimate $\delta^{13}C$ and $\delta^{18}O$ in CO emission based on combustion efficiency. However, more experiments and error bars are needed. $\delta^{13}C$ of OC fraction in carbonaceous aerosols shows some correlation with $\delta^{13}C$ in CO, but in what condition such correlation exists remains uncertain. Fuel moisture

in general does not show significant effect on emissions. At what stage and to what extent fuel moisture content impacts emission remain unclear. This study may not be able to realistically simulate various fuel moisture contents. VOC emission ratios in this study have large spread and mean emission ratio to CO_2 between different sets of experiments vary greatly and far lower than that of typical forest.

References

Akagi, S. K., Yokelson, R. J., Wiedinmyer, C., Alvarado, M. J., Reid, J. S., Karl, T., Crounse, J. D., and Wennberg, P. O.: Emission factors for open and domestic biomass burning for use in atmospheric models, Atmos. Chem. Phys., 11, 4039–4072, https://doi.org/10.5194/acp-11-4039-2011, 2011.

Alencar, A., Asner, G. P., Knapp, D., and Zarin, D.: Temporal variability of forest fires in eastern Amazonia, Ecol. Appl., 21, 2397–2412, doi: 10.1890/10-1168.1, 2011.

Andreae, M. O. and Rosenfeld, D.: Aerosol–cloud– precipitation interactions, Part 1, The nature and sources of cloud-active aerosols, Earth-Sci. Rev., 89, 13–41, doi: 10.1016/j.earscirev.2008.03.001, 2008.

Basu, S., Clerbaux, C., and Peters, W.: Response of the Amazon carbon balance to the 2010 drought derived with CarbonTracker South America, Global Biogeochem. Cy., 29, 1092–1108, doi:10.1002/2014GB005082, 2015.

Bergamaschi et al., 2000 P. Bergamaschi, R. Hein, C.A.M. Brenninkmeijer, P.J. Crutzen Inverse modeling of the global CO cycle: 2. Inversion of 13C/12C and 18O/16O isotope ratios J. Geophys. Res.: Atmospheres, 105, 1929-1945, doi: 10.1029/1999JD900819, 2000

Bowman, D. M. J. S., Balch, J. K., Artaxo, P., Bond,W. J., Carlson, J. M., Cochrane, M. A., D'Antonio, C. M., DeFries, R., Doyle, J. C., Harrison, S. P., Johnston, F. H., Keeley, J. E., Krawchuk, M. A., Kull, C. A., Marston, J. B., Mortiz, M. A., Prentice, I. C., Roos, C. I., Scott, A. C., Swetnam, T. W., van der Werf, G. R., and Pyne, S. J.: Fire in the Earth System, Science, 324, 481–484, doi:10.1126/science.1163886, 2009.

Brenninkmeijer, C. A. M., Röckmann, T., Bräunlich, M., Jöckel, P., and Bergamaschi, P.: Review of progress in isotope studies of atmospheric carbon monoxide, Chemosphere-Global Chang.Sci., 1, 33–52, doi: 10.1016/S1465-9972(99)00018-5,1999

Chen, L.-W. A., Verburg, P., Shackelford, A., Zhu, D., Susfalk, R., Chow, J. C., and Watson, J. G.: Moisture effects on carbon and nitrogen emission from burning of wildland biomass, Atmos. Chem. Phys., 10, 6617–6625, doi: 10.5194/acp-10-6617-2010, 2010.

Cofer, W. R., Winstead, E. L., Stocks, B. J., Overbay, L. W., Goldammer, J. G., Cahoon, D. R., and Levine, J. S.: 1996, 'Emissions from Boreal Forest Fires: Are the Atmospheric Impacts Underestimated?', in Levine, J. S. (ed.), Biomass Burning and Global Change, MIT Press, Cambridge, MA, pp. 834-839.

Crutzen, P. A. and Andreae, M. O.: Biomass burning in the tropics: Impact on atmospheric chemistry and biogeochemical cycles, Science, 250, 1669–1678, 1990.

Dominici F, Peng RD, Bell ML, Pham L, McDermott A, Zeger SL et al., Fine particulate air pollution and hospital admission for cardiovascular and respiratory diseases. JAMA, 295:1127-113416522832, doi: 10.1001/jama.295.10.1127, 2006.

Fuzzi, S., Andreae, M. O., Huebert, B. J., Kulmala, M., Bond, T. C., Boy, M., Doherty, S. J., Guenther, A., Kanakidou, M., Kawamura, K., Kerminen, V.-M., Lohmann, U., Russell, L. M., and Pöschl, U.: Critical assessment of the current state of scientific knowledge, terminology, and research needs concerning the role of organic aerosols in the atmosphere, climate, and global change, Atmos. Chem. Phys., 6, 2017–2038, doi:10.5194/acp-6-2017-2006, 2006.

Gaeggeler, K., Pr´evˆot, A. S. H., Dommen, J., Legreid, G., Reimann, S., and Baltensperger, U.: Residential wood burning in an Alpine valley as a source for oxygenated volatile organic compounds, hydrocarbons and organic acids, Atmos. Environ., 42, 8278–8287, doi:10.1016/j.atmosenv.2008.07.038, 2008.

Kato, S., Akimoto, H., Rockmann, T., Braunlich, M., and Brenninkmeijer, C. A. M.: Stable isotopic compositions of carbon monoxide from biomass burning experiments, Atmos. Environ.,33, 4357–4362, doi:10.1016/S1352-2310(99)00243-5, 1999b.

Keeling, C. D.: The concentration and isotopic abundances of atmospheric carbon dioxide in rural areas, Geochim. Cosmochim. Ac., 13, 322–224, 1958.

van der Laan-Luijkx, I. T., van der Velde, I. R., Krol, M. C., Gatti, L. V., Domingues, L. G., Correia, C. S. C., Miller, J. B., Gloor, M., van Leeuwen, T. T., Kaiser, J. W., Wiedinmyer, C., Lelieveld, J., J. Evans, M. Fnais, D. Giannadaki, and A. Pozzer, The contribution of outdoor air pollution sources to premature mortality on a global scale, Nature, 525(7569), 367–371, doi: 10.1038/nature15371, 2015.

Manning et al., 1997 M.R. Manning, C.A.M. Brenninkmeijer, W. Allan Atmospheric carbon monoxide budget of the southern hemisphere: implications of 18O/12C measurements J. Geophys. Res.: Atmospheres, 102, 10673-10682, doi: 10.1029/96JD02743, 1997

Naus, S., Röckmann, T., & Popa, M. E., The isotopic composition of CO in vehicle exhaust. Atmospheric Environment, 177, 132-142, doi: 10.1016/j.atmosenv.2018.01.015, 2018.

Nepstad, D., Schwartzman, S., Bamberger, B., Santilli, M., Ray, D., Schlesinger, P., Lefebvre, P., Alencar, A., Prinz, E., Fiske, G., and Rolla, A.: Inhibition of Amazon deforestation and fire by parks and indigenous lands, Conserv. Biol., 20, 65–73, doi: 10.1111/j.1523-1739.2006.00351.x, 2006.

Pathirana, S.L., van der Veen, C., Popa, M.E., Röckmann, T., An analytical system for studying the stable isotopes of carbon monoxide using continuous flow-isotope ratio mass spectrometry (CF-IRMS). Atmospheric Measurement Techniques 8 (2), 2067–2092, doi: 10.5194/amt-8-5315-2015, 2015.

Reddington, C. L., Morgan, W. T., Darbyshire, E., Brito, J., Coe, H., Artaxo, P., Marsham, J., and Spracklen, D. V.: Biomass burning aerosol over the Amazon: analysis of aircraft, surface and satellite observations using a global aerosol model, Atmos. Chem. Phys. Discuss., doi: 10.5194/acp-2018-849, in review, 2018.

Robinson, A., Donahue, N., Shrivastava, M., Weitkamp, E., Sage, A., Grieshop, A., Lane, T., Pierce, J., and Pandis, S.: Rethinking organic aerosols: Semivolatile emissions and photochemical aging, Science, 315, 1259–1262, doi:10.1126/science.1133061, 2007.

Röckmann, T., C. A. M. Brenninkmeijer, G. Saueressig, P. Bergamaschi, J. N. Crowley, H. Fischer, and P. J. Crutzen, Mass-independent oxygen isotope fractionation in atmospheric CO as a result of the reaction CO + OH, Science, 281(5376), 544– 546, doi: 10.1126/science.281.5376.544, 1998.

Röckmann, T., P. Jockel, V. Gros, M. Braunlich, G. Possnert, and C. A. M. Brenninkmeijer ,Using 14C, 13C, 18O and 17O isotopic variations to provide insights into the high northern latitude surface CO inventory, Atmos. Chem. Phys., 2, 147– 159, doi: 10.5194/acp-2-147-2002, 2002.

Stevens, C. M., Kaplan, L., Gorse, R., Durkee, S., Compton, M., Cohen, S., and Bielling, K.: The kinetic isotope effect for carbon and oxygen in the reaction CO + OH, Int. J. Chem. Kinet., 12, 935–948, 1980doi: 10.1515/zna-1989-0505, 1989.

Ward, D. S., Kloster, S., Mahowald, N. M., Rogers, B. M., Randerson, J. T., and Hess, P. G.: The changing radiative forcing of fires: global model estimates for past, present and future, Atmos. Chem. Phys., 12, 10857–10886, doi: 10.5194/acp-12-10857-2012, 2012.

Wiedinmyer, C., Akagi, S. K., Yokelson, R. J., Emmons, L. K., Al-Saadi, J. A., Orlando, J. J., and Soja, A. J., The Fire INventory from NCAR (FINN): a high resolution global model to estimate the emissions from open burning: Geoscientific Model Development, 4, 625-641, doi:10.5194/gmd-4-625-2011, 2011.

van der Werf, G. R., J. T. Randerson, L. Giglio, N. Gobron, and A. J. Dolman (2008), Climate controls on the variability of fires in the tropics and subtropics, Global Biogeochem. Cycles, 22, GB3028, doi:10.1029/2007GB003122, 2008.

van der Werf, G. R., Randerson, J. T., Giglio, L., Collatz, G. J., Mu, M., Kasibhatla, P. S., Morton, D. C., DeFries, R. S., Jin, Y., and van Leeuwen, T. T.: Global fire emissions and the contribution of deforestation, savanna, forest, agricultural, and peat fires (1997-2009), Atmos. Chem. Phys., 10, 11707-11735, doi:10.5194/acp-10-11707-2010, 2010.

Yokelson, R. J., Bertschi, I. T., Christian, T. J., Hobbs, P. V., Ward, D. E., and Hao,W. M.: Trace gas measurements in nascent, aged, and cloud-processed smoke from African savanna fires by airborne Fourier transform infrared spectroscopy (AFTIR), J. Geophys. Res., 108, 8478, doi: 10.1029/2002JD002322, 2003.

Yokelson, R. J., Burling, I. R., Gilman, J. B., Warneke, C., Stockwell, C. E., de Gouw, J., Akagi, S. K., Urbanski, S. P., Veres, P., Roberts, J. M., Kuster, W. C., Reardon, J., Griffith, D. W. T., Johnson, T. J., Hosseini, S., Miller, J.W., Cocker III, D. R., Jung, H., and Weise, D. R.: Coupling field and laboratory measurements to estimate the emission factors of identified and unidentified trace gases for prescribed fires, Atmos. Chem. Phys., 13, 89–116, doi: 10.5194/acp-13-89-2013, 2013b.

Appendix

A Sample loops for CO isotope system

The newly implemented and tested part of the instrument is the sample loop inlet (provided by VICI® in Texas, USA). The advantage of sample loops is that only a small quantity of sample is needed for the measurement and thus samples of high concentration can be measured directly. With the sample loops, samples of high CO and CO_2 concentrations can be measured without time consuming dilution procedure beforehand. There are four sample loops that can be connected to the selector valve at a time. Possible choices for inner volumes of one sample loop include 5 µL, 25µL, 50µL, 250 µL, 1 mL (Table 12). The normal set-up is to include 5 µL, 25µL, 250 µL, 1 mL on the selector.

Table 12

Sample loop sizes, their theoretical equivalent dilution ratios for CO and CO_2 measurements and the maximum concentration of CO or CO_2 that can be measured in the sample

Sample loop size	Dilution ratio for CO	Max. [CO]	Dilution ratio for CO_2	Max. [CO_2]
5 µL	1:20000	1%	1:266	16%
25 µL	1:4000	2000 ppm	1:53	3.2%
50 µL	1:2000	1000 ppm	1:27	1.6%
250 µL	1:400	200 ppm	1:5.3	3180 ppm
1 mL	1:100	50 ppm	1:1.3	780 ppm